Hindawi
Geofluids
Volume 2021, Article ID 4366942, 16 pages
https://doi.org/10.1155/2021/4366942

Research Article

Disastrous Mechanism and Concentration Distribution of Gas Migration in Fully Mechanized Caving Stope in Wuyang Coal Mine

Li Chong,[1,2] He Sifeng,[1] and Xu Zhijun[1]

[1]*School of Mines, Key Laboratory of Deep Coal Resource Mining, Ministry of Education, China University of Mining and Technology, Xuzhou, 221116 Jiangsu, China*
[2]*School of Mines, Jiangsu Engineering Laboratory of Mine Earthquake Monitoring and Prevention, China University of Mining & Technology, Xuzhou, 221116 Jiangsu, China*

Correspondence should be addressed to He Sifeng; sifenghe541@163.com

Received 6 May 2021; Accepted 6 August 2021; Published 20 August 2021

Academic Editor: Yu Wang

Copyright © 2021 Li Chong et al. This is an open access article distributed under the Creative Commons Attribution License, which permits unrestricted use, distribution, and reproduction in any medium, provided the original work is properly cited.

The overrunning disaster of harmful gas tends to occur in the working face in thick coal seam with high gas concentration, as the fully mechanized caving stope has the characteristics of high mining intensity, high remnant coal, and high gas content. Therefore, the disastrous mechanism and concentration distribution of gas migration in fully mechanized caving stope are the theoretical basis for gas control scheme. Based on the 7607 working face in Wuyang coal mine, the gas emission quantity in working face is comprehensively analyzed by field measurement in this paper. The gas leakage field, oxygen concentration field, and gas concentration field in 7607 working face are simulated by establishing the equal proportional numerical model. Due to the increase of air leakage in working face caused by the high alley pumping drainage, the risk of coal spontaneous combustion is also analyzed, when gas extraction in goaf is carried out. The research results show that the gas drainage technology in high drainage roadway has a remarkable effect on the gas overrunning phenomenon. The gas concentration near the upper corner of the working surface has been reduced from 0.7%-1% to 0.5%. At the same time, it is necessary to pay attention to the risk of coal spontaneous combustion in the goaf for gas drainage in the high drainage roadway. The width of the oxidation zone in the goaf is about 25 m deeper than that before the drainage. Research results provide the references for gas control technology and coal spontaneous combustion prevention in similar working faces.

1. Introduction

Gas overrunning disaster not only directly threatens the safety of coal miners but also restricts the production capacity in coal mine [1, 2]. The coal output of fully mechanized caving stope is large, while the gas emission is uneven [3–5]. Meanwhile, the gas concentration in fully mechanized caving stope changes greatly in a short time, which is easy to cause gas accidents [6, 7]. Long-term production practice shows that gas migration and gas concentration distribution are important parts of gas control in fully mechanized caving stope [8–10]. For coal mine with complex production conditions, such as high gas and thick coal seams, it is particularly important to understand the gas migration status in the working face and choose a reasonable gas control scheme [11–13]. Only by figuring out the factors affecting the gas concentration in fully mechanized caving stope can the occurrence of gas disaster be prevented, and the high yield and high efficiency of the mine be realized. Therefore, it is necessary to carry out the research on the disastrous mechanism and concentration distribution of gas migration in fully mechanized caving stope.

The gas outburst from the goaf to the working face is one of the main reasons for the gas overrunning disaster [14–16]. In high-gas mines, there are more remnant coal in goaf with low-position top coal caving mining technology, and the gap between the remnant coal is large [17, 18]. Therefore, after gas is gushing out, it is easy to flow through the goaf and flow

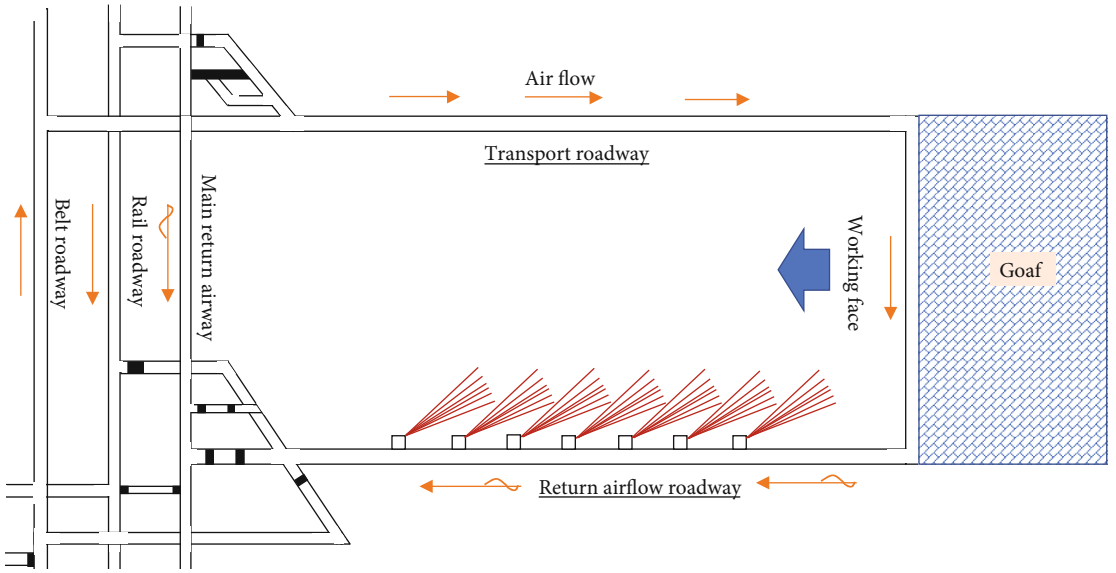

Figure 1: Schematic diagram in 7607 working face.

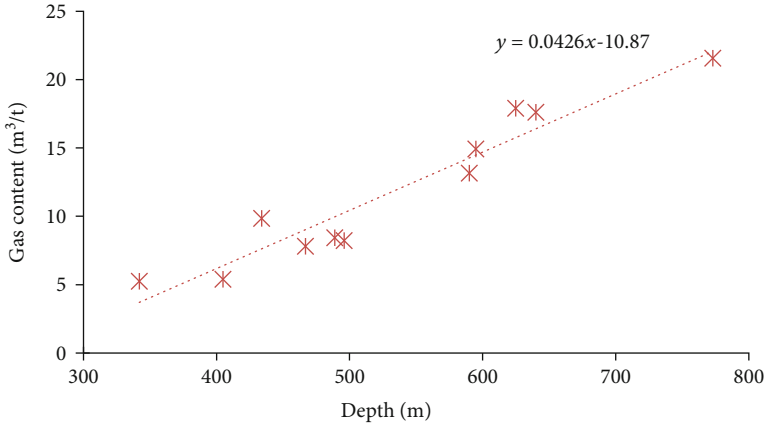

Figure 2: The relationship between the gas content and the buried depth of the 3# coal seam.

under the drive of air pressure. In the "U" type ventilation working face, when the air flow enters the stope from the inlet roadway, the gas in the goaf brings out to the working face, causing the gas concentration in the working face [19–21].

The gas drainage technology in high drainage roadway is widely used in China, which plays a good role in preventing the overrunning of gas concentration in the working face [22, 23]. For the working face in coal seam with high gas and spontaneous combustion, gas extraction through high drainage roadway alleviates the gas emission disaster but increases the air leakage in the working face to a certain extent and accelerates the process of spontaneous combustion of remnant coal in goaf [24, 25]. Xia et al. [26] studied the disaster mechanism of coexistence of gas and coal spontaneous combustion and the action mechanism of coupling effect. Chu et al. [27] analyzed the disturbance effect of roof roadway gas drainage on goaf spontaneous combustion area.

Therefore, it is of practical significance to study the characteristics of air leakage and the distribution of three zones for the prevention and control of coal spontaneous combustion in goaf. Therefore, aiming at the problem of gas overrunning in the high gas fully mechanized caving stope, this paper adopts the actual production conditions in the 7607 working

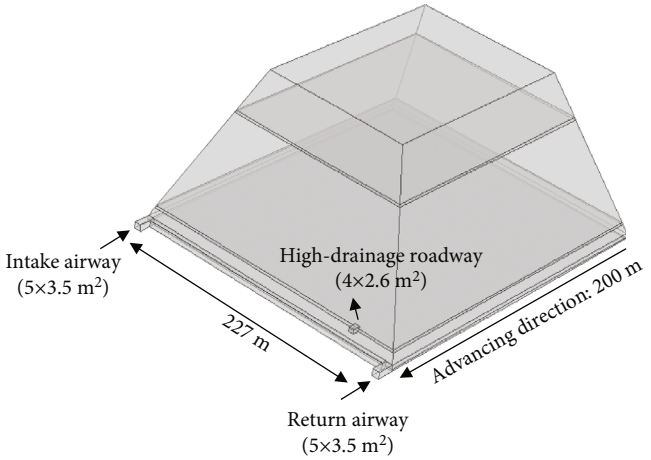

Figure 3: Numerical calculation model of 7607 working face.

Figure 4: Schematic diagram of mesh division.

Table 1: Numerical simulation parameters.

Mark	Value	Meaning
rho_CH4	0.717 (kg/m^3)	Gas density under standard condition
rho_air	1.29 (kg/m^3)	Air density
D	1*e*-5 (m^2/s)	Gas diffusion coefficient
Mug	1.8e-5 (Pa*s)	Gas dynamic viscosity
pn	-2 (KPa)	Pressure at return air exit
Gp_c	260 (m^3/min)	Extraction quantity of high pumping roadway
k0	1.45	Natural expansion coefficient
k1	1.15	Residual expansion coefficient
u0	5.1 (m/s)	Flow velocity of intake airflow roadway
u_15	5*e*-7 (m/s)	Gas emission rate of residual coal in goaf
u_14	8*e*-7 (m/s)	Gas emission rate of adjacent coal seam
v_mol	22.4 (l/mol)	Molar volume of gas
M_O2	32 (g/mol)	Molar mass of oxygen
M_N2	28 (g/mol)	Molar mass of nitrogen
M_CH4	16 (g/mol)	Molar mass of methane

face in Wuyang coal mine and analyzes the gas emission situation by field measurement in the working face.

2. Gas Occurrence Law in 7607 Working Face

2.1. Basic Overview of Mining Area and Working Face. Wuyang coal mine is a large modern mine of Lu'an Group, which is located in Xiangyuan County, Changzhi City, Shanxi Province. It is about 13 km long from north to south and 10 km wide from east to west, covering an area of 78.3649 km^2. There are thirteen coal seams in the minefield, including two mineable seams, one most mineable seam, and ten locally and occasionally mineable seams, with a total thickness of 13.31 m and a coal content coefficient of 8.17%. Among them, 3# coal seam is located in the middle and lower part of Shanxi formation, with an average thickness of 5.75 m. The whole area is generally stable, which is the coal seam being mined. The ventilation mode in Wuyang coal mine is divided into diagonal type, and the ventilation method is the extraction type.

The layout of 7607 working face in Wuyang coal mine is shown in Figure 1. Fully mechanized top coal caving is adopted in the working face, which has the characteristics of high yield and high efficiency. However, due to high mining intensity, fast advancing speed, and large gas emission in the working face, it is easy to cause gas overrunning in the upper corner or mine return air roadway, which brings great potential safety hazard for production.

2.2. Law of Gas Occurrence in Working Face. Fitting the gas content measured in Wuyang coal mine to the buried depth of the coal seam, the relationship between the gas content of the coal seam and the buried depth of the coal seam is obtained. The corresponding relationship between the gas content in the 3# coal seam and the buried depth is shown in Figure 2.

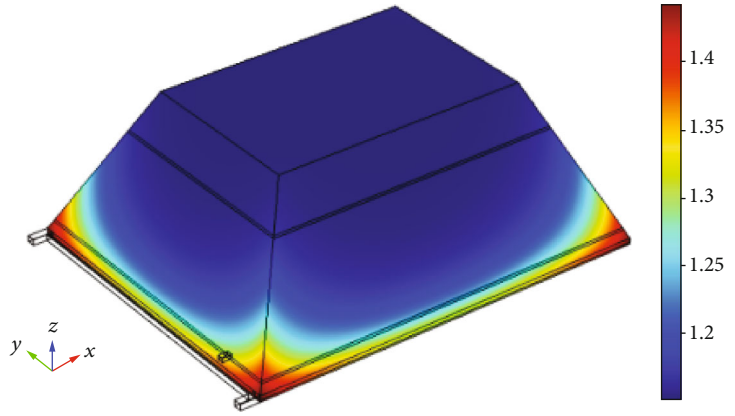

(a) Expansion coefficient

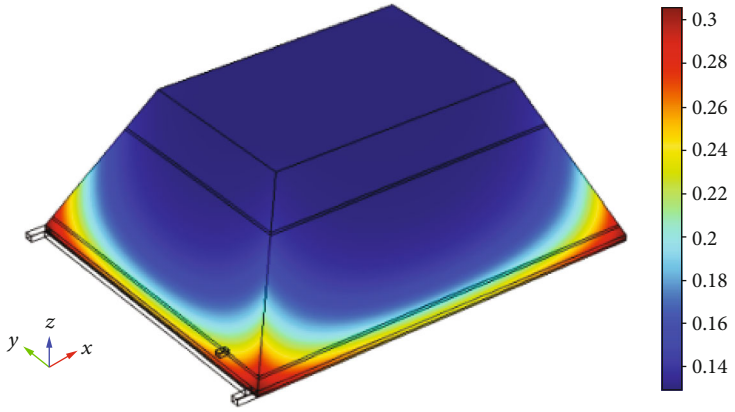

(b) Porosity

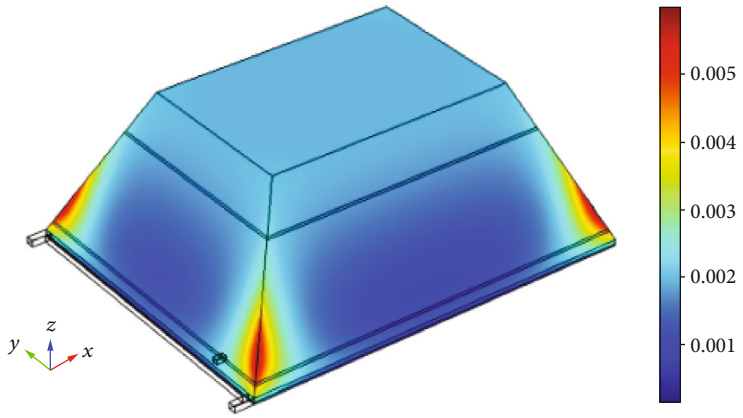

(c) Permeability coefficient (m^2)

Figure 5: Continued.

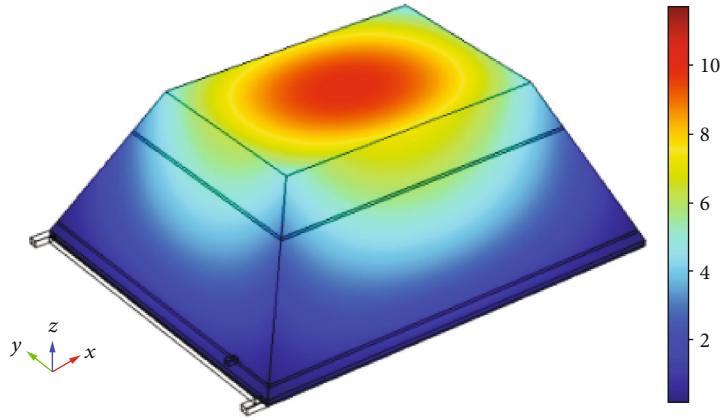

(d) Stress distribution (N/m^2)

Figure 5: Distribution of seepage parameters in goaf.

The buried depth of coal seam at 7607 working face in Wuyang Coal Mine is 512 m-593 m. According to the formula of relation between gas content and buried depth, the coal seam gas content at 7607 working face is calculated to be 10.63 m^3/t-13.95 m^3/t.

3. Gas Migration Law and Coal Spontaneous Combustion Risk under *U*-Type Ventilation

3.1. Numerical Calculation Model. The 7607 working face adopts the comprehensively top coal mining technology scheme, with the open-cut length of 227 m and the advancing length of 1002 m. The average depth of coal seam in the working face is 600 m, and the thickness is 6.06 m, and the mining height is 3 m, and the coal discharge is 3 m, and the raw coal gas content in the working face is 9.1 m^3/t, and the air distribution volume is 4000 m^3/min. On the basis of the *U*-shaped ventilation scheme, the 7607 working face adopts gas drainage technology in high drainage roadway. Taking the intersection of the return airway and the working face as the origin of the coordinates in the COMSOL numerical analysis software, the direction of mined-out area is the x -axis direction, and the inclination is the y-axis direction, and the vertical direction is the z-axis direction to establish the geometric model, as shown in Figure 3. The section size of intake airway and return airway is 17.5 m^2 (5 m × 3.5 m). The section size of high drainage roadway is 10.4m^2 (4 m × 2.6 m).

According to the actual situation in the 7607 working face, the strike length of the model is 200 m, and the inclination length is 227 m. The mesh of the working face area in the numerical calculation model is encrypted, shown in Figure 4. Tetrahedral mesh is used for mesh generation, the total number of meshes is 6×10^5, and mesh encryption is carried out at the working face.

The intake airflow roadway is the entrance of speed, and the return air roadway is the free flow, and the high suction roadway is the mass exit, and the four sides which contact the high suction roadway and the goaf are the interface. The gas emission law in working face, the air leakage flow field in goaf, the distribution law of oxygen concentration field, and gas concentration field are calculated. The numerical simulation parameters are shown in Table 1.

According to the mass conservation equations, the momentum conservation equations, and the diffusion motion equations, the mathematical model of oxygen and gas transport in the working face and the mined-out area is established, combined with the actual conditions in fully mechanized caving stope. The numerical simulation software COMSOL is employed to solve the model.

3.2. Distribution of Seepage Parameters in Goaf. Under the effect of air leakage pressure difference in goaf, the air flows between these pores. The surface of coal adsorbs the oxygen in the air leakage and reacts with it to form spontaneous combustion, which is the main reason for spontaneous combustion of residual coal in goaf. The distribution of porosity in goaf is closely related to the lithology of coal roof, compressive strength of coal seam, and distribution of mine pressure in goaf. The distribution of seepage parameters in goaf is shown in Figure 5.

Due to the collapse of the overlying strata in the goaf, the stress distribution in the goaf meets the "O" ring distribution theory. At the end of the working face and two roadway positions, the coefficient of coal and rock crushing expansion and porosity and permeability are larger, while the coefficient of coal and rock fragmentation and porosity and permeability are smaller in the middle of the goaf due to stress compaction. In order to further analyze the gas seepage environment in the goaf, the seepage parameters at the position of $z = 1.5$ m at the floor of the goaf are further extracted, shown in Figure 6.

There are some differences in the distribution of seepage parameters in different positions of goaf. From the goaf near the end of the working face and two roadways, the porosity is larger, and the porosity in the middle and deep is smaller. Due to the collapse of overlying strata, the crushing expansion coefficient, porosity, and permeability at the inlet and return air roadway near the working face and the upper and lower angle of the deep solid wall boundary of the goaf are all large; the influence range is about 20 m. The porosity near the end of working face reaches the maximum value of

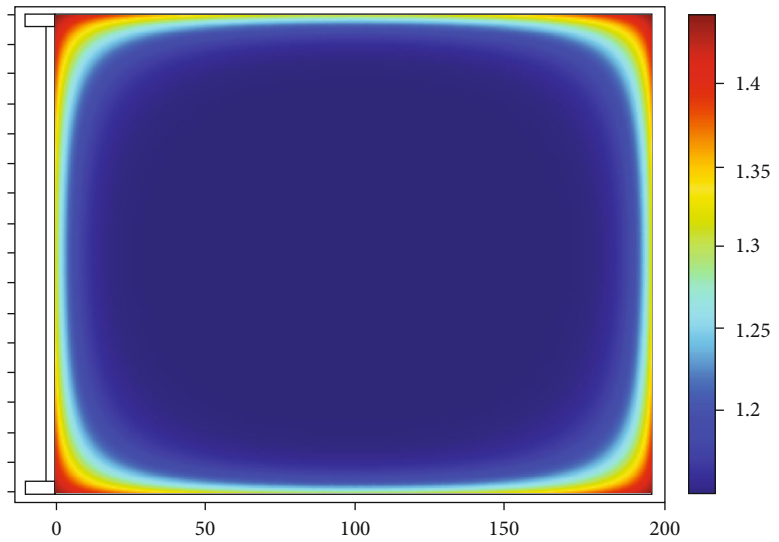

(a) Expansion coefficient

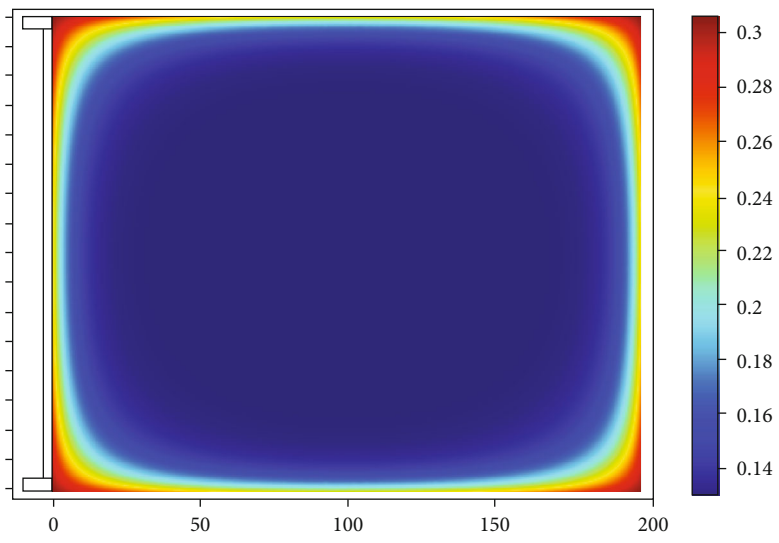

(b) Porosity

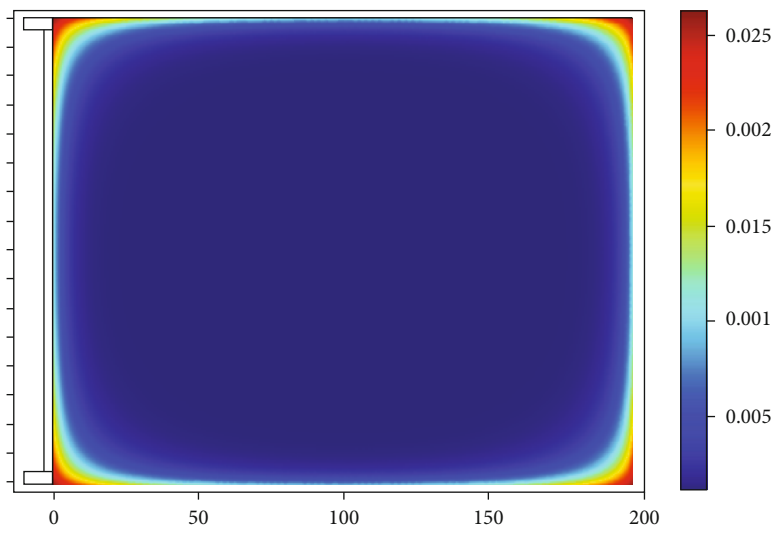

(c) Permeability coefficient (m^2)

Figure 6: Continued.

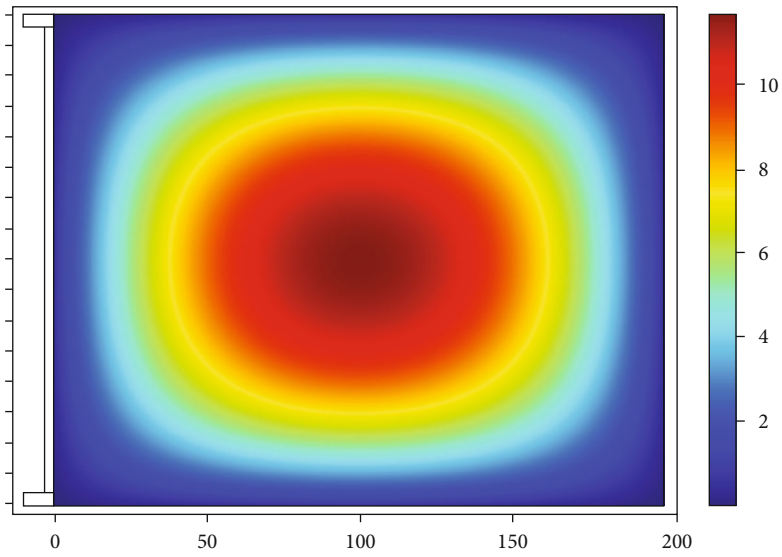

(d) Stress distribution (N/m^2)

Figure 6: Distribution of seepage parameters at $z = 1.5$ m of goaf floor.

0.3 at the inlet and return air. The stress distribution of the goaf reaches the maximum in the middle of the goaf and decreases with the extension of the wall around the goaf.

3.3. Distribution of Flow Field and Concentration Field in Goaf. The change of gas composition in goaf, especially the content of oxygen and gas, depends on the distribution of air leakage and airflow. Therefore, the study of goaf seepage flow is an important theoretical basis for residual coal spontaneous combustion and gas emission and accumulation. The study of goaf seepage distribution provides an important basis for the study of goaf gas distribution and residual coal spontaneous combustion. When the inlet air volume is 4000 m^3/min, the distribution of air leakage velocity at the floor $z = 1.5$ m of goaf is shown in Figure 7.

The air leakage rate in the goaf is relatively large at about 20 m near the end of the working face on the strike in Figure 7(a). When it reaches 50 m deep into the goaf, the air leakage rate gradually decreases and is less than 1 m/min. The reason for this phenomenon is the "O" circle distribution of coal mass in goaf. With the development of mining, the roof of goaf collapses. Therefore, there are a lot of air leakage into the goaf in the upper and lower corners in the goaf. The oxygen concentration distribution in the goaf is uneven in Figure 7(b). Due to the velocity inertia of the air leakage flow on the inlet side, the oxidation depth on the inlet side is greater than that on the return side.

In order to analyze the law of gas distribution in the stope and effectively control the gas level in the working face, the three-dimensional gas concentration distributions in goaf and floor are shown in Figures 7(c) and 7(d). Due to the dilution effect of the air leakage flow on the gas in the goaf, the gas concentration in the air inlet side is significantly lower than that in the air return side. Because the influence scope of air leakage is limited, the dilution effect of air flow on gas is relatively weak, when it reaches the middle and deep part of goaf. Therefore, the gas concentration in the middle and deep part of goaf is higher.

3.4. Division of Spontaneous Combustion Oxidation Zone in Goaf. In order to further analyze the location of spontaneous combustion oxidation zone in goaf, the "three zones" in the goaf are divided by 0.004 m/s (0.24 m/min) and 0.001 m/s (0.1 m/min). The distribution range of spontaneous combustion oxidation zone based on air leakage wind speed is shown in Figure 8(a). The spontaneous combustion oxidation zone in goaf is distributed in the range of 50 m-150 m behind the goaf. On the inlet and return wind side, the isoline of 0.004 m/s is deep to about 120 m in the goaf strike. Based on the analysis of the distribution law of oxygen concentration in goaf, the oxygen concentration contour with $z = 1.5$ m at the floor is extracted for analysis, in order to clearly understand the distribution pattern of spontaneous combustion oxidation zone in goaf.

The distribution of oxidation zone in goaf with 18%-10% oxygen concentration as the division index is shown in Figure 8(b). The white area near the working face is the tropical zone, the colored area between 18% and 10% oxygen concentration contour is the spontaneous combustion zone, and the area with oxygen concentration less than 10% is the asphyxiation zone. When the spontaneous combustion zone extends from the air inlet side of the goaf to the air return side of the goaf, its width gradually decreases. The width of the oxidation zone on the air return side of the goaf is relatively narrow, compared with the central part of the goaf and the air inlet side. In one side of the inlet roadway, the range of spontaneous combustion zone is 75 m-160 m, and the width of spontaneous combustion zone is 85 m, and the width of spontaneous combustion zone is 85 m. The spontaneous combustion zone in the middle of goaf is 85 m-150 m, and the width of spontaneous combustion zone is 65 m. The range of spontaneous combustion zone on one side of the

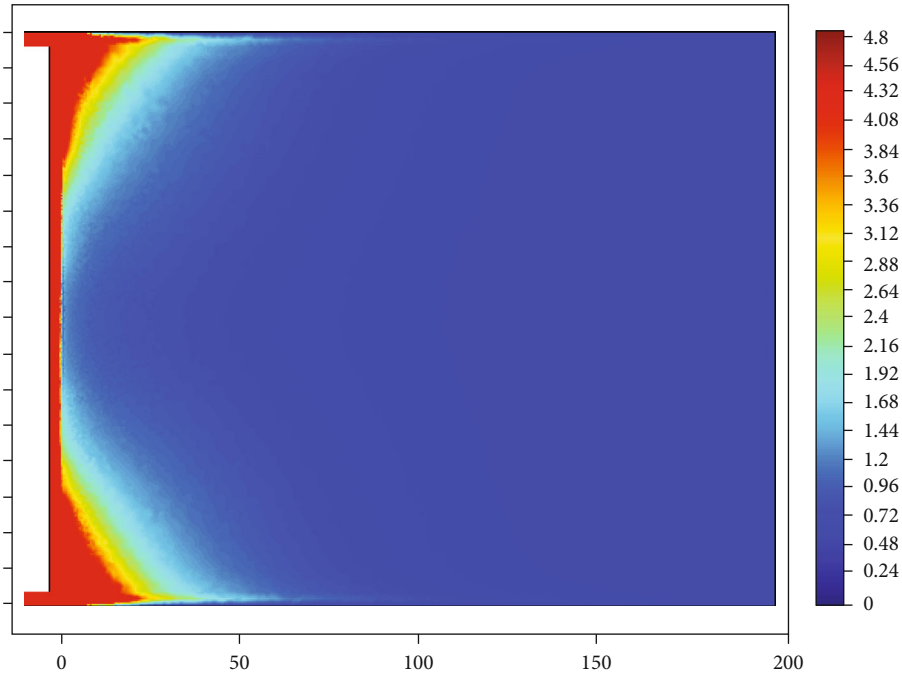

(a) Air leakage velocity

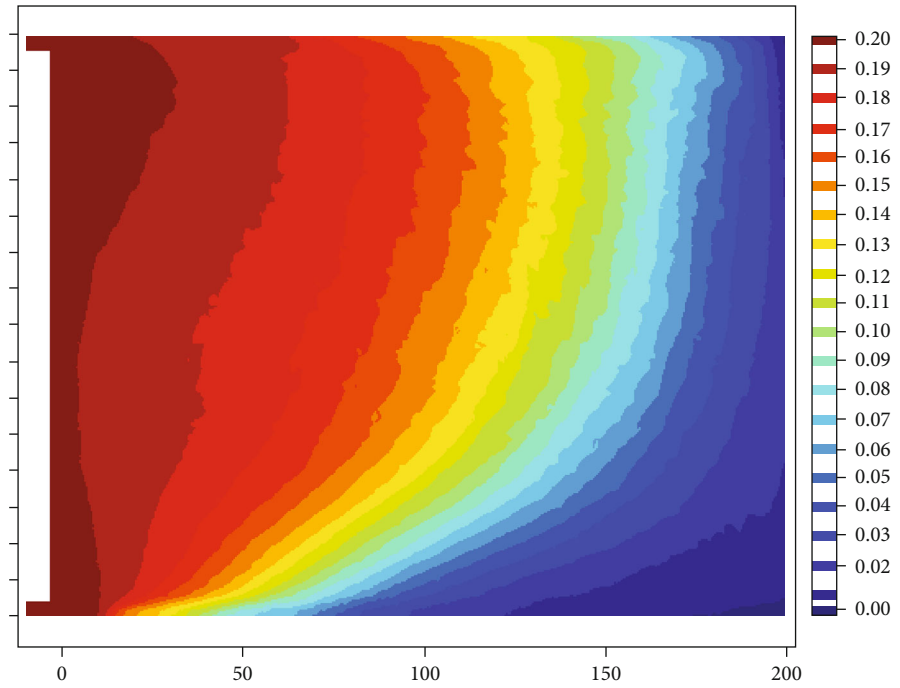

(b) Distribution of oxygen density

Figure 7: Continued.

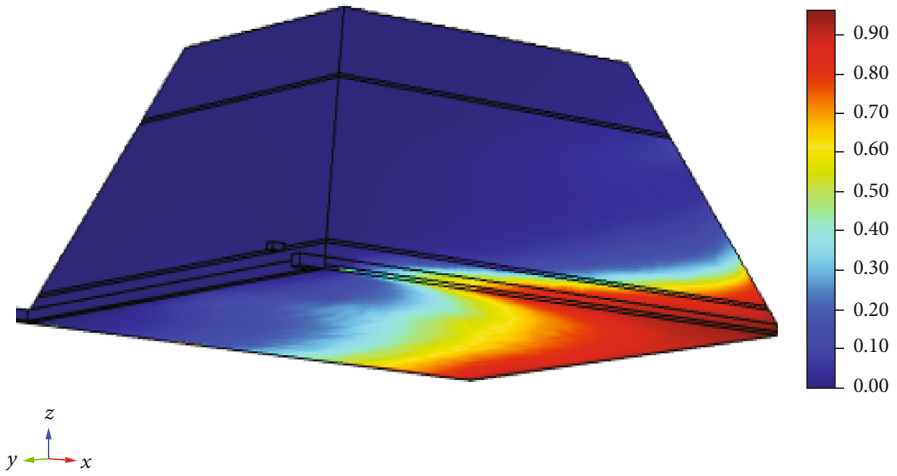

(c) Gas concentration distribution in goaf

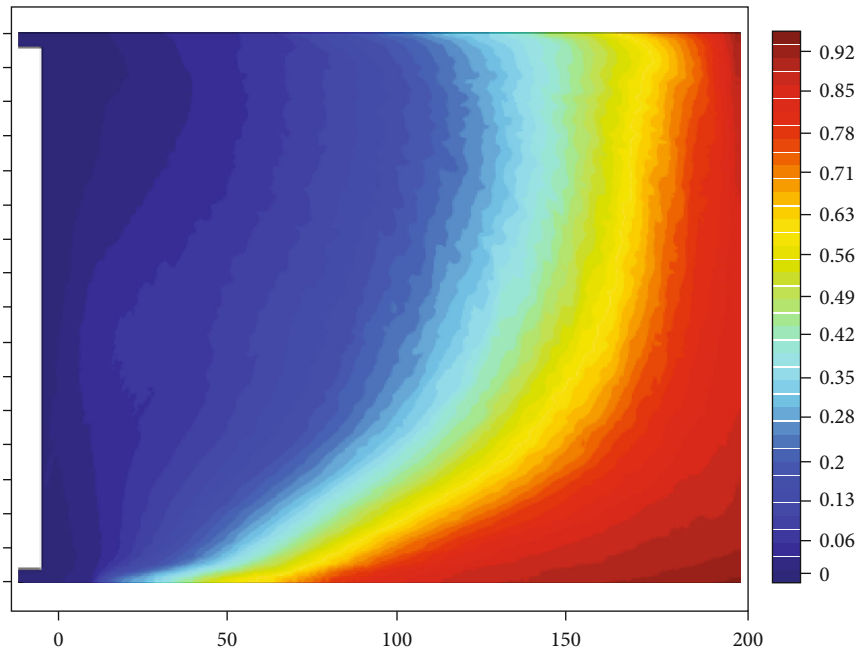

(d) Gas concentration distribution in floor

Figure 7: Distribution of flow field and concentration field at $z = 1.5$ m of goaf floor.

return air roadway is 20 m-45 m, and the width of spontaneous combustion zone is 25 m. Combined with the oxidation zone range divided by air leakage wind speed and oxygen concentration, the oxidation zone range is determined to be 20 m-150 m, in order to reduce the risk of coal spontaneous combustion in goaf.

4. Multicomponent Gas Migration and Coal Spontaneous Combustion Risk under the Condition of High Pumping Roadway

4.1. The Distribution of Flow Field and Concentration Field in Goaf. In order to further control the gas level in the goaf, gas extraction is carried out in the high pumping roadway above the roof of the goaf, and the extraction rate is 260 m^3/min. Firstly, the air leakage velocity distribution at $z = 1.5$ m in the goaf floor under the condition of high pumping roadway is shown in Figure 9(a). In order to further analyze the change rule of oxygen concentration on the inlet and outlet side under the action of high pumping roadway, the changes of oxygen concentration at 30 m away from the inlet and outlet side are extracted, shown in Figure 9(b). The oxygen concentration at the air inlet side drops to 18% after entering the goaf about 110 m, and the oxygen concentration at the air inlet side about 170 m is 10%. The three-dimensional gas concentration distribution in goaf under the effect of high pumping roadway is shown in Figure 9(c). In order to clearly understand the gas concentration distribution in working face and goaf, the contour map of gas concentration at the goaf floor $z = 1.5$ m is extracted, shown in Figure 9(d).

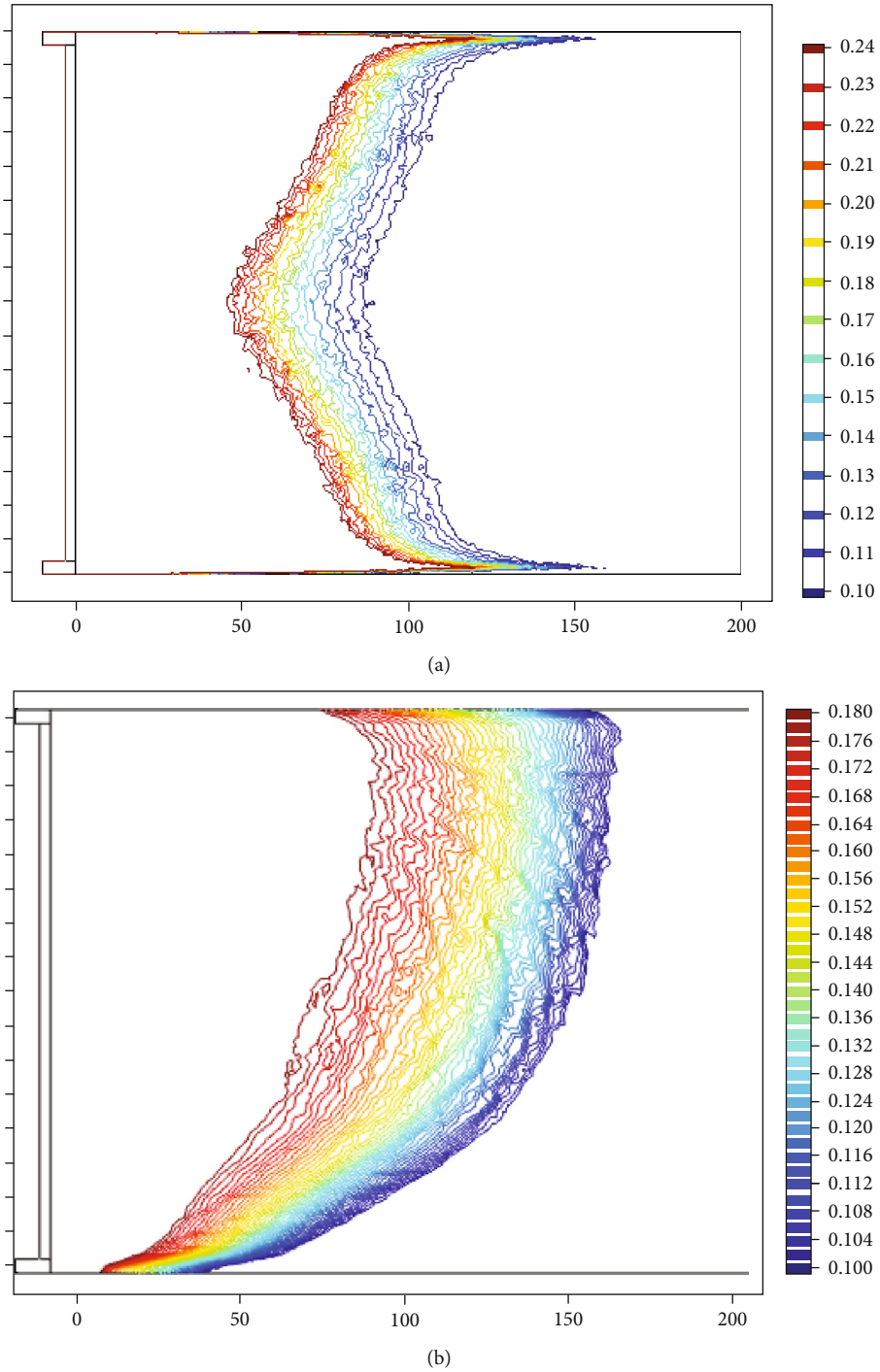

Figure 8: Distribution of oxidation zone at $z = 1.5$ m of goaf floor.

4.2. Division of Spontaneous Combustion Oxidation Zone in Goaf. Compared with the leakage field under *U*-shaped ventilation, the air leakage velocity range at the return air corner becomes larger due to the influence of gas extraction in the high pumping roadway; especially, the air leakage velocity at the position of the return air roadway is significantly increased. The three-zone distribution of goaf under the condition of gas extraction in high pumping roadway is shown in Figure 10(a), which is divided by air leakage speed as an indicator. The spontaneous combustion oxidation zone in goaf is distributed in the range of 60 m-160 m behind goaf. The red area is the tropic zone, the blue area is the suffocation zone, and the gradient area between them is the spontaneous combustion oxidation zone. Compared with the distribution of air leakage velocity under *U*-type ventilation, the depth of oxidation zone in goaf under high extraction roadway is larger. On the inlet and return wind side, the 0.24 m/min isoline is deep to about 140 m of the goaf strike. In Figure 11(b),

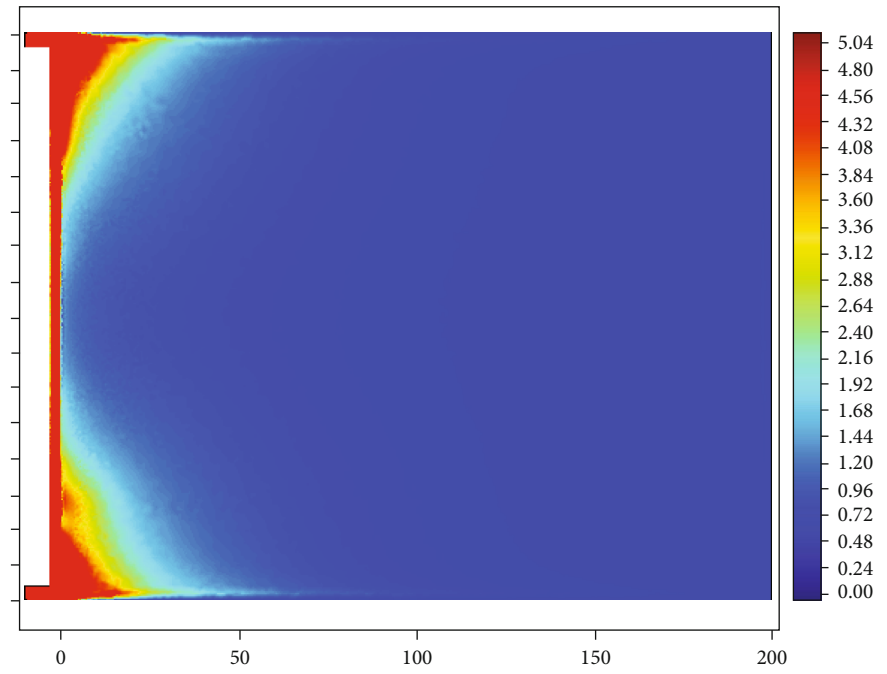

(a) Air leakage velocity

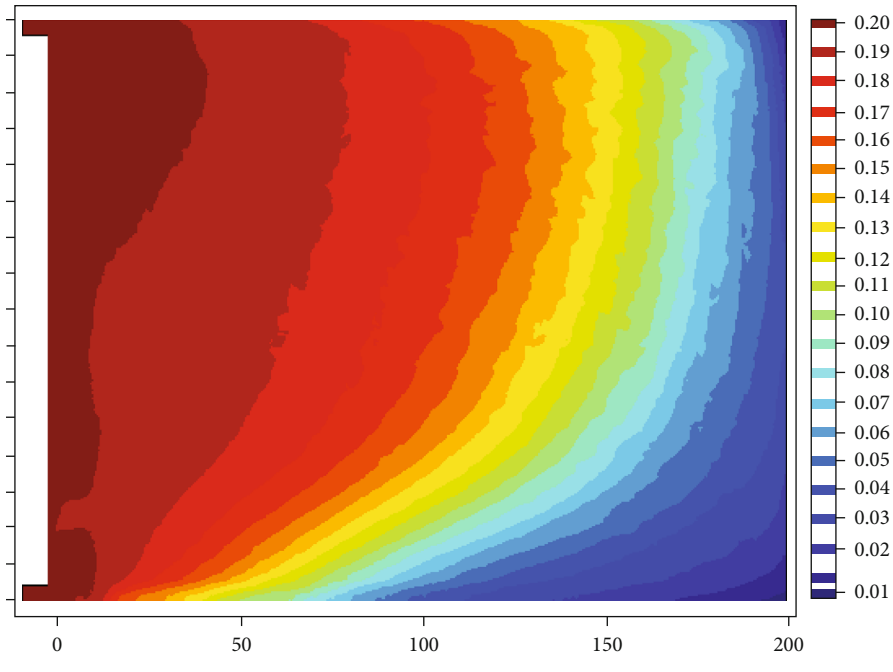

(b) Distribution of oxygen density

Figure 9: Continued.

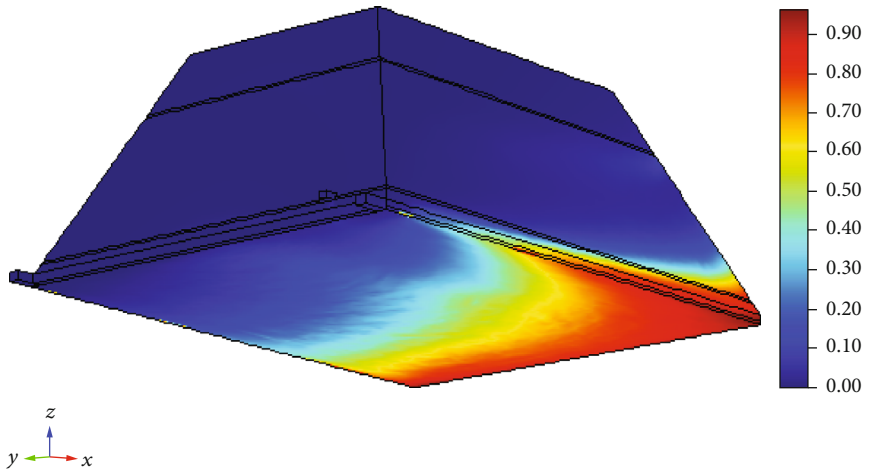

(c) Gas concentration distribution in goaf

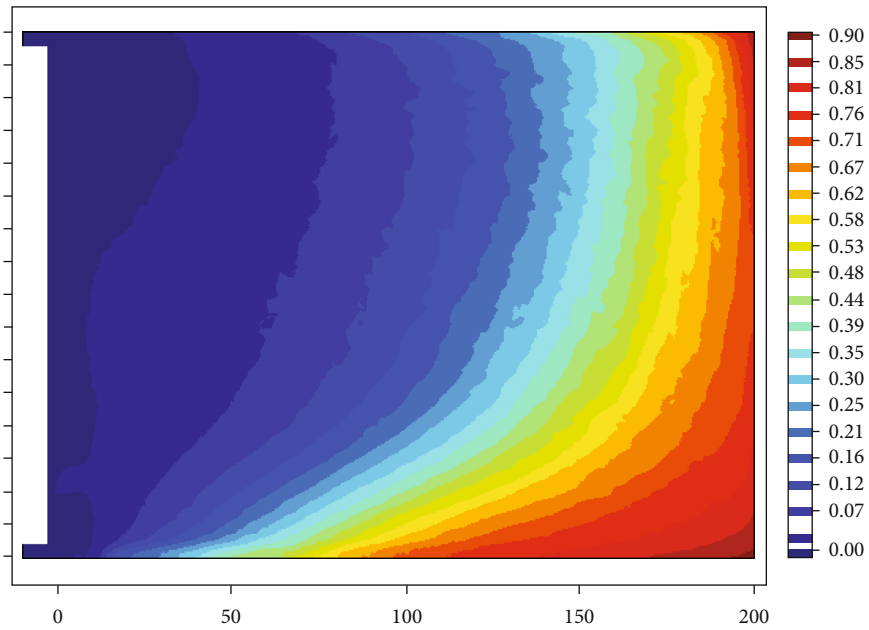

(d) Gas concentration distribution in floor

Figure 9: Distribution of flow field and concentration field at $z = 1.5$ m in the goaf floor under the condition of high pumping roadway.

the white area near the working face is the scattered tropical zone, the colored area between the 18% and 10% oxygen concentration contour lines is the spontaneous combustion zone, and the area with oxygen concentration less than 10% is the asphyxiation zone. The range of spontaneous combustion zone on one side of the air inlet roadway is 90 m-175 m in Figure 10(b), and the width of spontaneous combustion zone is 85 m; the range of spontaneous combustion zone in the middle of the goaf is 100 m-160 m, and the width of spontaneous combustion zone is 60 m; the range of spontaneous combustion zone on one side of the air return roadway is 20 m-75 m, and the width of spontaneous combustion zone is 55 m.

Compared with the *U*-type ventilation, the width of oxidation zone at the inlet side and the middle of goaf has little change, and the oxidation depth moves back about 10 m. The 18% isoline of the oxidation zone on the return side changes little, and the 10% isoline moves backward obviously. The width of oxidation zone on the return air side changed greatly, which increased by 30 m compared with the previous 25 m width.

4.3. Comparison of Oxygen and Gas Concentration in Goaf before and after Gas Drainage in High Drainage Roadway. The volume fraction of oxygen and gas on both sides of air intake airway and air return airway in goaf before and after gas extraction in high drainage roadway is compared, as shown in Figures 11 and 12. It can be seen from Figure 11 that the air leakage in goaf is increased after gas extraction in high drainage roadway, and the oxygen volume fraction in the inlet and return air side is increased significantly. When the depth of goaf is 50 m, the oxygen volume fraction at the inlet airway and return airway side increases by 2% and 5%, respectively. Gas drainage in high drainage roadway

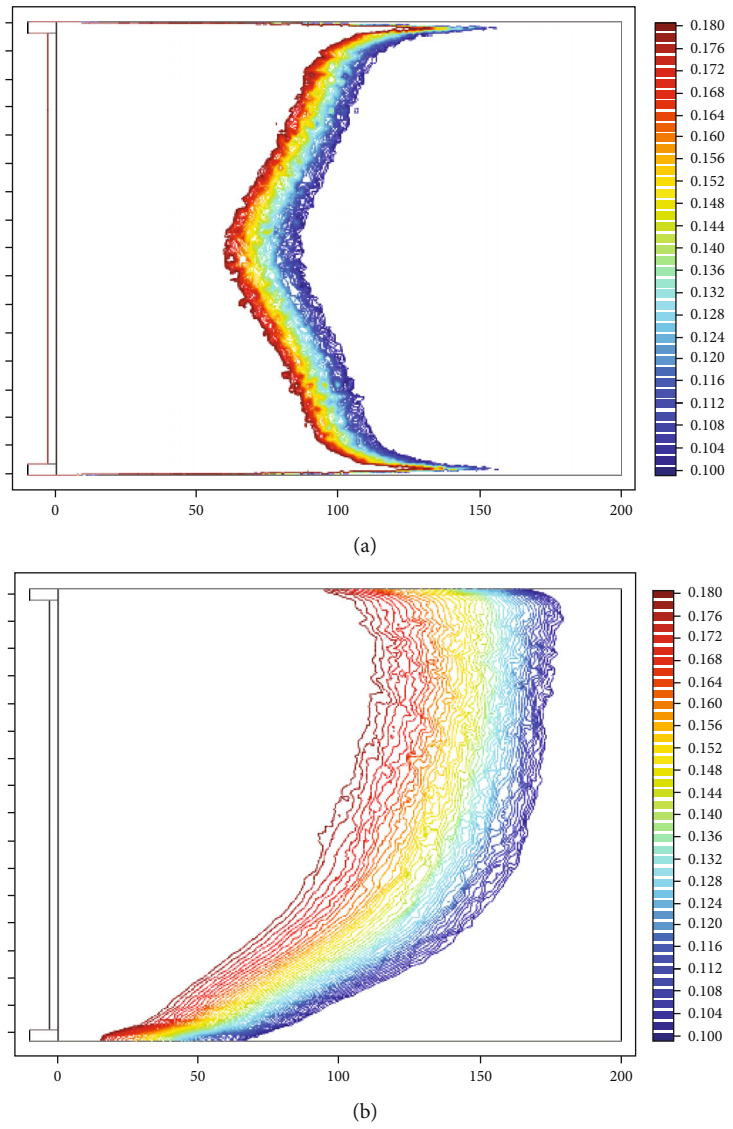

Figure 10: Distribution of oxidation zone at $z = 1.5$ m in goaf floor.

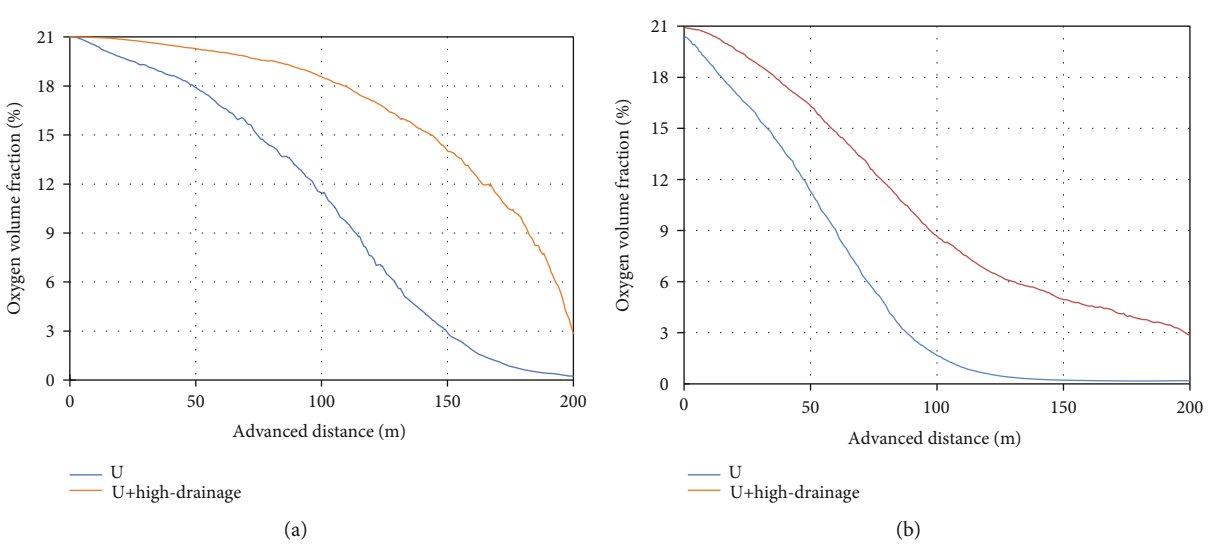

Figure 11: Volume fraction of oxygen in intake (a) and return (b) airway before and after high drainage.

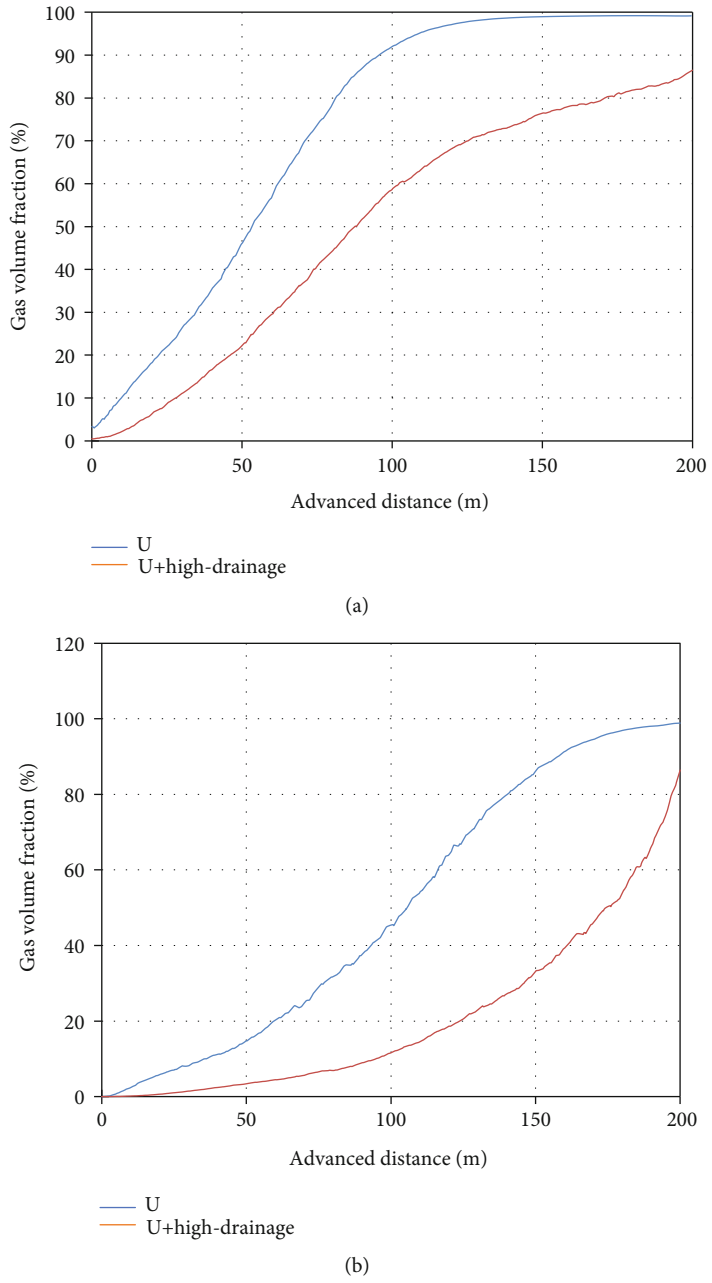

Figure 12: Volume fraction of gas in intake (a) and return (b) airway before and after high drainage.

obviously reduces the gas volume fraction in goaf, and the gas volume fraction on both sides of inlet and return airway decreases obviously, as shown in Figure 12. When the depth of goaf is 50 m, the gas volume fraction at the air inlet and air return side decreases by 10% and 20%, respectively. Especially, the gas concentration near the upper corner of the working face is obviously reduced, which effectively inhibits the gas emission from the goaf to the working face.

5. Conclusions

(1) The buried depth of coal seam is the key factor affecting gas occurrence. The relationship between coal seam gas content and coal seam buried depth is obtained, the growth gradient of gas content is 4.2 m^3/t/hm, and the coal seam gas content in the 7607 working face is predicted to be 10.63 m^3/t-13.95 m^3/t. Through the measurement of gas content, it is proved that the gas occurrence law is consistent with the actual situation

(2) The measured gas emission from the coal wall and falling coal mass in the working face is 26.09 m^3/min, the gas entering the goaf with air leakage is 1.12 m^3/min, and the air leakage in the working face is 581 m^3/min. The simulation results show that the range of spontaneous combustion oxidation zone

in goaf in 7607 working face is 50 m-160 m at the inlet roadway side, 50 m-150 m at the central goaf, and 20 m-150 m at the return air roadway side

(3) By measuring the gas accumulation concentration in different areas in the working face and determining the natural oxidation zone (seepage area) in goaf in numerical simulation, the gas accident area is comprehensively determined. Through the gas control effect monitoring, it is confirmed that the gas concentration in the upper corner of the fully mechanized top coal caving stope in Wuyang coal mine is not more than 0.8%, and the gas concentration in the return air roadway is not more than 0.8%.

Data Availability

The data used to support the findings of this study are included within the article.

Conflicts of Interest

The authors declare that they have no conflicts of interest.

Acknowledgments

The study was supported by the National Natural Science Foundation of China (51874277).

References

[1] Y. Cao, Y. Li, and Z. Zhou, "Spatial-temporal variation features and law of gas concentration in the fully mechanized working face under the condition of intermittent ventilation," *International Journal of Mining Science and Technology*, vol. 29, no. 6, pp. 963–969, 2019.

[2] L. Zhu, F. Dang, Y. Xue, K. Jiao, and W. Ding, "Multivariate analysis of effects of microencapsulated phase change materials on mechanical behaviors in light-weight aggregate concrete," *Journal of Building Engineering*, vol. 42, article 102783, 2021.

[3] H. Wang, X. Yang, F. Du et al., "Calculation of the diffusion coefficient of gas diffusion in coal: the comparison of numerical model and traditional analytical model," *Journal of Petroleum Science and Engineering*, vol. 205, article 108931, 2021.

[4] F. Du and K. Wang, "Unstable failure of gas-bearing coal-rock combination bodies: insights from physical experiments and numerical simulations," *Process Safety and Environmental Protection*, vol. 129, pp. 264–279, 2019.

[5] W. L. Shen, J. B. Bai, W. F. Li, and X. Y. Wang, "Prediction of relative displacement for entry roof with weak plane under the effect of mining abutment stress," *Tunnelling and Underground Space Technology*, vol. 71, pp. 309–317, 2018.

[6] L. Cheng, L. Shugang, and Y. Shouguo, "Gas emission quantity prediction and drainage technology of steeply inclined and extremely thick coal seams," *International Journal of Mining Science and Technology*, vol. 28, no. 3, pp. 415–422, 2018.

[7] Y. Xue, F. Gao, Y. Gao, X. Liang, Z. Zhang, and Y. Xing, "Thermo-hydro-mechanical coupled mathematical model for controlling the pre- mining coal seam gas extraction with slotted boreholes," *International Journal of Mining Science and Technology*, vol. 27, no. 3, pp. 473–479, 2017.

[8] H. W. Zhou, H. P. Xie, and J. P. Zuo, "Development in researches on mechanical behaviors of rocks under the condition of high ground pressure in the depths," *Advances in Mechanics*, vol. 1, pp. 91–99, 2005.

[9] Y. Xue, T. Teng, F. Dang, Z. Ma, S. Wang, and H. Xue, "Productivity analysis of fractured wells in reservoir of hydrogen and carbon based on dual-porosity medium model," *International Journal of Hydrogen Energy*, vol. 45, no. 39, pp. 20240–20249, 2020.

[10] D. Ma, H. Duan, W. Liu, X. Ma, and M. Tao, "Water–sediment two-phase flow inrush hazard in rock fractures of overburden strata during coal mining," *Mine Water and the Environment*, vol. 39, no. 2, pp. 308–319, 2020.

[11] B. H. Yao, Z. Chen, J. Wei, T. Bai, and S. Liu, "Predicting erosion-induced water inrush of karst collapse pillars using inverse velocity theory," *Geofluids*, vol. 2018, Article ID 2090584, 18 pages, 2018.

[12] F. Du, K. Wang, X. Zhang, C. Xin, L. Shu, and G. Wang, "Experimental study of coal-gas outburst: insights from coal-rock structure, gas pressure and adsorptivity," *Natural Resources Research*, vol. 29, no. 4, pp. 2481–2493, 2020.

[13] L. L. Si, J. Wei, Y. Xi et al., "The influence of long-time water intrusion on the mineral and pore structure of coal," *Fuel*, vol. 290, article 119848, 2021.

[14] Z. Z. Cao, P. Xu, Z. H. Li, M. X. Zhang, Y. Zhao, and W. L. Shen, "Joint bearing mechanism of coal pillar and backfilling body in roadway backfilling mining technology," *CMC-Computers Materials & Continua*, vol. 54, no. 2, pp. 137–159, 2018.

[15] Y. Xue, P. G. Ranjith, F. Dang et al., "Analysis of deformation, permeability and energy evolution characteristics of coal mass around borehole after excavation," *Natural Resources Research*, vol. 29, no. 5, pp. 3159–3177, 2020.

[16] Z. Z. Cao, F. Du, Z. H. Li, Q. T. Wang, P. Xu, and H. X. Lin, "Research on instability mechanism and type of ore pillar based on the fold catastrophe theory," *CMES-Computer Modeling in Engineering & Science*, vol. 113, no. 3, pp. 287–306, 2017.

[17] Y. Xue, J. Liu, F. Dang, X. Liang, S. Wang, and Z. Ma, "Influence of CH_4 adsorption diffusion and CH_4-water two-phase flow on sealing efficiency of caprock in underground energy storage," *Sustainable Energy Technologies and Assessments*, vol. 42, article 100874, 2020.

[18] X. X. Miao, H. Pu, and H. B. Bai, "Principle of water-resisting key strata and its application in water-preserved mining," *Journal of China University of Mining and Technology*, vol. 1, pp. 1–4, 2008.

[19] M. G. Qian and J. L. Xu, "Study on the "O shape" circle distribution characteristics of mining induced fracture in the overburden strata," *Journal of China Coal Industry*, vol. 5, pp. 20–23, 1998.

[20] L. L. Si, H. Zhang, J. Wei, B. Li, and H. Han, "Modeling and experiment for effective diffusion coefficient of gas in water-saturated coal," *Fuel*, vol. 284, article 118887, 2021.

[21] Z. Z. Cao, Y. Ren, Q. Wang, B. Yao, and X. Zhang, "Evolution mechanism of water-conducting channel of collapse column in karst mining area of southwest China," *Geofluids*, vol. 2021, Article ID 6630462, 8 pages, 2021.

[22] D. Ma, J. Wang, and Z. Li, "Effect of particle erosion on mining-induced water inrush hazard of karst collapse pillar,"

Environmental Science and Pollution Research, vol. 26, no. 19, pp. 19719–19728, 2019.

[23] S. G. Li, C. S. Li, H. F. Lin, and L. H. Cheng, "Technique of drawing relieved methane and simultaneous extraction of coal and coakbed methane," *Journal of Xi'an University of Science and Technology*, vol. 263, pp. 247–249, 2002.

[24] Y. Xue, J. Liu, P. G. Ranjith, X. Liang, and S. Wang, "Investigation of the influence of gas fracturing on fracturing characteristics of coal mass and gas extraction efficiency based on a multi-physical field model," *Journal of Petroleum Science and Engineering*, vol. 206, article 109018, 2021.

[25] Y. P. Cheng, J. H. Fu, and Q. X. Fu, "Development of gas extraction technology in coal mines of China," *Journal of Mining and Safety Engineering*, vol. 23, pp. 127–139, 2009.

[26] T. Q. Xia, F. Zhou, X. Wang et al., "Controlling factors of symbiotic disaster between coal gas and spontaneous combustion in longwall mining gobs," *Fuel*, vol. 182, pp. 886–896, 2016.

[27] T. X. Chu, M. Yu, and D. Jiang, "Experimental investigation on the permeability evolution of compacted broken coal," *Transport in Porous Media*, vol. 116, no. 2, pp. 847–868, 2017.